

# Lattice parameters, deviations from Vegard's rule, and $E_2$ phonons in InAlN

V. Darakchieva,<sup>1,2,a)</sup> M.-Y. Xie,<sup>2</sup> F. Tasnádi,<sup>2</sup> I. A. Abrikosov,<sup>2</sup> L. Hultman,<sup>2</sup> B. Monemar,<sup>2</sup> J. Kamimura,<sup>3</sup> and K. Kishino<sup>3,4</sup>

<sup>1</sup>Instituto Tecnológico e Nuclear, 2686-953 Sacavém, Portugal

<sup>2</sup>IFM, Linköping University, SE-581 83 Linköping, Sweden

<sup>3</sup>Department of Engineering and Applied Sciences, Sophia University, Tokyo 102-8554, Japan

<sup>4</sup>CREST, Japan Science and Technology Agency, Japan

(Received 30 October 2008; accepted 5 December 2008; published online 31 December 2008)

The lattice parameters of  $\text{In}_x\text{Al}_{1-x}\text{N}$  in the whole compositional range are studied using first-principle calculations. Deviations from Vegard's rule are obtained via the bowing parameters,  $\delta_a=0.0412 \pm 0.0039 \text{ \AA}$  and  $\delta_c=-0.060 \pm 0.010 \text{ \AA}$ , which largely differ from previously reported values. Implications of the observed deviations from Vegard's rule on the In content extracted from x-ray diffraction are discussed. We also combine these results with x-ray diffraction and Raman scattering studies on  $\text{In}_x\text{Al}_{1-x}\text{N}$  nanocolumns with  $0.627 \leq x \leq 1$  and determine the  $E_2$  phonon frequencies versus In composition in the scarcely studied In-rich compositional range. © 2008 American Institute of Physics. [DOI: 10.1063/1.3056656]

Recently,  $\text{In}_x\text{Al}_{1-x}\text{N}$  alloys have attracted considerable research interest due to the large energy range covered by their band gaps from 0.6 eV (InN) to 6 eV (AlN). In addition,  $\text{In}_x\text{Al}_{1-x}\text{N}$  thin films with In content  $x=0.17\text{--}0.20$  allow lattice-matching to GaN and have been extensively studied in relation to their application for Bragg reflectors, microcavities, and field-effect transistors.<sup>1,2</sup> Despite the intense investigations on  $\text{In}_x\text{Al}_{1-x}\text{N}$ , many of the material properties, in particular, for In-rich alloys, remain unexplored or controversial, e.g., lattice parameters, phonons, and band gap energies. The possible deviations from Vegard's rule in InAlN have also been a subject of ongoing discussions,<sup>3–6</sup> but consensus has not been achieved yet.

In this work we report a study on the lattice parameters of  $\text{In}_x\text{Al}_{1-x}\text{N}$  using first-principle calculations and discuss the observed deviations from Vegard's rule and their implications for the In composition extracted from x-ray diffraction (XRD). In order to calibrate  $E_2$  phonon frequencies versus In composition we also combine these results with XRD and Raman scattering studies on In-rich  $\text{In}_x\text{Al}_{1-x}\text{N}$  nanocolumns.

First-principle calculations were performed by using the Vienna *ab initio* simulation program<sup>7</sup> with the projector augmented-wave method and Perdew–Burke–Ernzerhof generalized gradient approximation (GGA) for the exchange–correlation potential. The In  $4d$  orbitals were treated as valence states. The disorder problem was treated by means of a supercell approach with a special quasirandom distribution of In and Al atoms on the metal sublattice.<sup>8</sup> The  $(4 \times 2 \times 4)$  supercells were generated as described in Ref. 9 and represented to be a very good model along the entire composition range by showing vanishing Warren–Cowley short-range order parameters up to the seventh neighboring shells.

Figure 1(a) shows the calculated relaxed lattice parameters of  $\text{In}_x\text{Al}_{1-x}\text{N}$  versus In composition  $x$ . The calculated lattice parameters for pure InN ( $a=3.589 \text{ \AA}$  and  $c=5.793 \text{ \AA}$ ) and AlN ( $a=3.131 \text{ \AA}$  and  $c=5.012 \text{ \AA}$ ) are in good agreement with previously reported experimental values,<sup>10,11</sup> being slightly larger. The GGA overestimation of the lattice parameters is 0.6% (1.5%) for AlN (InN), which lies in the typical

(0%–3%) range. Both  $c$  and  $a$  lattice parameters exhibit essentially a linear dependence on the In composition with very small deviations from Vegard's rule [Fig. 1(a)]. The variation of the  $\text{In}_x\text{Al}_{1-x}\text{N}$  lattice parameters with In content  $x$  [Fig. 1(a)] can be approximated by

$$\xi(x) = x\xi^{\text{InN}} + (1-x)\xi^{\text{AlN}} - \delta_\xi x(1-x), \xi = a, c, \quad (1)$$

where  $\delta_a=0.0412 \pm 0.0039 \text{ \AA}$  and  $\delta_c=-0.060 \pm 0.010 \text{ \AA}$  describe the deviations from Vegard's rule. Our  $\delta_a$  and  $\delta_c$

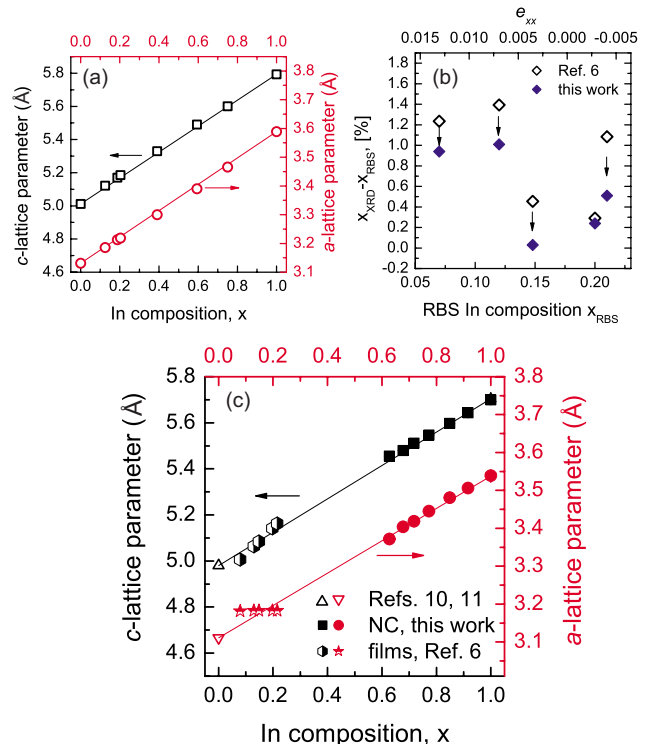


FIG. 1. (Color online) (a) Calculated equilibrium lattice parameters  $a$  and  $c$  of  $\text{In}_x\text{Al}_{1-x}\text{N}$  vs In composition,  $x$ ; (b) differences between the XRD and RBS in contents in thin  $\text{In}_x\text{Al}_{1-x}\text{N}$  films assuming validity of Vegard's rule (Ref. 6) and taking into account the deviations from Vegard's rule,  $\delta_a=0.0412 \text{ \AA}$  and  $\delta_c=-0.060 \text{ \AA}$ , obtained in this work; (c) experimental lattice constants  $a$  and  $c$ , in  $\text{In}_x\text{Al}_{1-x}\text{N}$  nanocolumns (NC) vs In composition  $x$ , accounting for  $\delta_a=0.0412 \text{ \AA}$  and  $\delta_c=-0.060 \text{ \AA}$ . The lattice parameters of InN (Ref. 10) and AlN (Ref. 11) powder and thin  $\text{In}_x\text{Al}_{1-x}\text{N}$  films (Ref. 6) are given for comparison.

<sup>a)</sup>Electronic mail: vanya@ifm.liu.se.

values are smaller than the previously calculated  $\delta_a = 0.063 \pm 0.014 \text{ \AA}$  and  $\delta_c = -0.16 \pm 0.015 \text{ \AA}$ ,<sup>3</sup> which however are based on calculations using  $(2 \times 2 \times 1)$  supercells. In this respect, we note that our  $(4 \times 2 \times 4)$  supercells mimic the short-range order parameters providing a more accurate model of the perfectly random alloy. The GGA overestimation of the lattice parameters in the In rich range has only a negligible effect (below the error bars) on the deduced bowing parameters.

Although small,  $\delta_a$  and  $\delta_c$  should be accounted for in the composition extracted by XRD. Strain-free InAlN alloys in the form of nanostructures are envisioned for future optoelectronic applications. In such strain-free alloys, the extracted composition from the  $c$  lattice parameter will be overestimated by more than 1% for  $x \leq 0.6$  if  $\delta_c$  is not taken into account. We note that an overestimation of the In content as large as 2% can be observed around the compositional range for lattice matching to GaN. If the  $a$  lattice parameter is used to extract the In content in  $\text{In}_x\text{Al}_{1-x}\text{N}$  without taking into account  $\delta_a$ , an underestimation close to 1% can be expected in the lattice-matched range, and may deviate by as much as 3% for  $0.2 \leq x \leq 0.8$ .

The situation is more complicated for  $\text{In}_x\text{Al}_{1-x}\text{N}$  films, which are under strain due to the heteroepitaxial growth. In this case the proper extraction of the In composition requires to separate the effect of strain on the lattice parameters (see, for example, Ref. 6). For thick  $\text{In}_x\text{Al}_{1-x}\text{N}$  films grown on GaN buffers with composition close to the lattice matching to GaN, and thus with low degree of strain<sup>6</sup> any intrinsic deviations from Vegard's rule would be treated erroneously as biaxial strain in the extraction of the XRD composition (Refs. 4 and 6) if  $\delta_a$  and  $\delta_c$  are not accounted for. In such case, the deviations from the actual composition remain below 0.5%. This result is in agreement with our previous observation that there is reasonable agreement between the In contents determined by XRD assuming validity of Vegard's rule and Rutherford back scattering (RBS) for such relaxed layers close to the lattice matching composition. The error in the XRD In content associated with the assessment of strain<sup>6</sup> can be well represented by the difference between RBS and XRD results, because of the intrinsic insensitivity of the RBS content to strain. An accuracy of 0.3% in the RBS In content can be achieved.

On the other hand, we previously observed larger deviations between the XRD and RBS In contents for highly strained  $\text{In}_x\text{Al}_{1-x}\text{N}$  films when the XRD content is extracted assuming validity of Vegard's rule [Fig. 1(b)]. Better agreement or in other words reduced error in the XRD In content is achieved if  $\delta_a$  and  $\delta_c$  obtained in this work are accounted for as demonstrated in Fig. 1(b). However, the remaining smaller differences in the In contents still seem to be correlated with the strain in the films. This suggests that the uncertainties in the stiffness constants of InN and AlN, as well as in the strain-free lattice parameters, are the limiting factors to achieve better precision in the XRD composition. A deviation from the linear dependence of the stiffness constants with In content, which is assumed when taking into account the effect of strain may also contribute. We caution that in general a hydrostatic strain component may be present in In-rich  $\text{In}_x\text{Al}_{1-x}\text{N}$  films, e.g., due to unintentional impurities or N overstoichiometry. If not accounted for it will lead to erroneous XRD In content. It is worth noting that the devia-

tions from Vegard's rule have also consequences for the magnitude of the strain and the respective lattice-matched composition, which can critically affect device characteristics and design. For instance, the difference in the strain reaches as much as 2.5 times and the lattice-matched composition differs by 1.4% when the deviations are accounted for in the thin films discussed in Fig. 1(b).

Furthermore, we measured the lattice parameters of (002)-oriented In-rich  $\text{In}_x\text{Al}_{1-x}\text{N}$  nanocolumns with diameters of 100–200 nm for  $x < 1$  and 1000 nm for  $x = 1$ . The samples were grown by molecular beam epitaxy (MBE) on GaN buffered sapphire in the case of pure InN and on Si substrates for  $x < 1$ , all exhibiting strong photoluminescence at room temperature.<sup>12</sup> The  $c$  and  $a$  lattice parameters of the  $\text{In}_x\text{Al}_{1-x}\text{N}$  nanocolumns were determined from the 002 and 101  $2\theta$ - $\omega$  XRD spectra, respectively. We obtain for pure InN nanocolumns  $c = 5.7002 \pm 0.0001 \text{ \AA}$  and  $a = 3.5390 \pm 0.0011 \text{ \AA}$  in very good agreement with  $c = 5.7037 \pm 0.0004 \text{ \AA}$  and  $a = 3.5377 \pm 0.0002 \text{ \AA}$  measured for InN powder by synchrotron XRD.<sup>10</sup> In the form of powder, the materials cannot sustain any microstrains, and therefore their lattice parameters present good estimate for the strain-free case. Hence, the observed closeness between our lattice parameters of the InN nanocolumns and those of InN powder indicates only a negligible degree of strain in the nanocolumns. This result is in agreement with previous findings for group-III nitride nanocolumns grown by MBE.<sup>13</sup> We then adopted the method described in Ref. 6 to extract the In composition in the nanocolumns and take into account the deviations from Vegard's rule obtained in this work. The estimated compositions in the  $\text{In}_x\text{Al}_{1-x}\text{N}$  nanocolumns vary between  $x = 1$  and  $x = 0.627$ , and the results are shown in Fig. 1(c). For comparative reasons, we also plotted in Fig. 1(c) the results on the lattice parameters determined in our previous work,<sup>6</sup> but taking into account  $\delta_a$  and  $\delta_c$  when extracting the XRD composition. It is seen that the nanocolumns remain very close to the strain-free state for the compositional range studied  $0.627 \leq x \leq 1$ , in contrast to the thin films exhibiting noticeable strain [Fig. 1(c)].

We now turn to the  $E_2$  phonon mode behavior in the  $\text{In}_x\text{Al}_{1-x}\text{N}$  nanocolumns. The  $E_2$  phonon in group-III nitrides is Raman active and its frequency in alloys depends on the alloy composition and degree of strain, but it is not affected by free carriers due to the nonpolar nature of the mode. Therefore, the  $E_2$  phonon frequency is often the tool of choice to calibrate strain or composition in semiconducting alloy heterostructures since it presents a nondestructive and fast way to access them. The experimental studies on phonons in  $\text{In}_x\text{Al}_{1-x}\text{N}$  are scarce,<sup>15,16</sup> focusing on the Al-rich range (up to  $x = 0.7$ ) and suffering from the uncertainties in the composition as discussed above. In the  $\text{In}_x\text{Al}_{1-x}\text{N}$  nanocolumns the effects of strain are minimized and thus the compositional dependence of the  $E_2$  phonon frequency can be established in the poorly studied In-rich compositional range.

Figure 2(a) shows representative Raman spectra of the nanocolumns for three different In compositions. The experiment was conducted at room temperature in  $z(x)\bar{z}$  backscattering configuration with the  $x$ -direction parallel to the  $c$ -axis of the nanocolumns. The 514.5 nm line of an Ar<sup>+</sup> laser was used for excitation and the spectral resolution was  $1 \text{ cm}^{-1}$ . The spectra were collected at multiple sample loca-

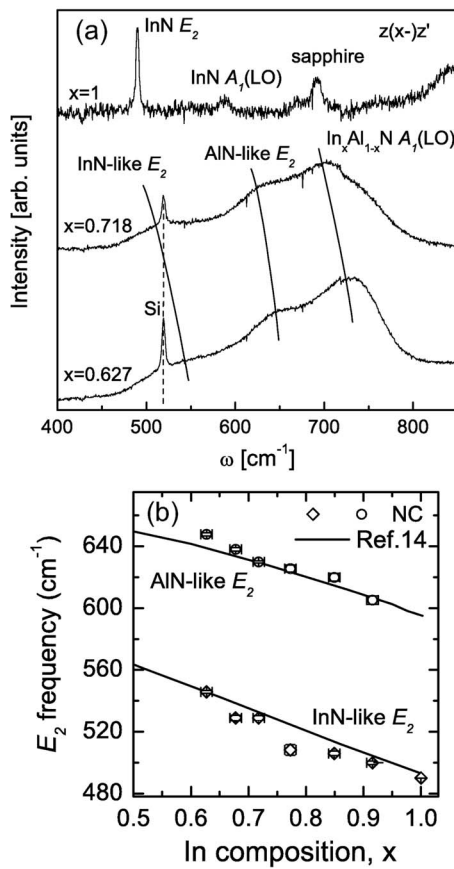


FIG. 2. (a) Representative Raman scattering spectra from the  $\text{In}_x\text{Al}_{1-x}\text{N}$  nanocolumns with highest  $x=1$ , intermediate  $x=0.718$ , and lowest  $x=0.627$  In content; (b) InN-like and AlN-like  $E_2$  frequency shifts vs the In content in the nanocolumns (NC). The theoretical predictions (Ref. 14) are also shown for comparison.

tions and the data scatter, weighted by the errors from the fits, is used as error bar. The allowed  $\text{In}_x\text{Al}_{1-x}\text{N}$   $E_2$  and  $A_1$  longitudinal optical (LO) phonons are detected for all samples [Fig. 2(a)] in agreement with the selection rules. We found that the  $\text{In}_x\text{Al}_{1-x}\text{N}$   $E_2$  phonons exhibit two-mode behavior, while the  $A_1$  (LO) shows one-mode behavior as predicted by theory.<sup>14</sup> The  $A_1$  (LO) structure becomes more prominent for lower-In content nanocolumns [Fig. 2(a)] as a result of near-resonant enhancement due to Fröhlich electron-phonon interaction with LO phonons.

The  $E_2$  frequency was determined to be  $490.0 \pm 0.1 \text{ cm}^{-1}$  for the pure InN nanocolumns in good agreement with the strain-free frequency of  $491.1 \text{ cm}^{-1}$  estimated in our previous study on compact InN films with different degrees of strain.<sup>17</sup> The full width at half maximum of the InN  $E_2$  phonon is only  $2.3 \text{ cm}^{-1}$  evidencing the high crystalline quality of the InN nanocolumns as confirmed by XRD. Figure 2(b) shows the InN-like and AlN-like  $E_2$  phonon frequencies in the  $\text{In}_x\text{Al}_{1-x}\text{N}$  nanocolumns versus the In content. The redshift of the experimental InN-like  $E_2$  frequencies with respect to the theoretical line was previously observed also for InGaN and the reasons are not well understood. A blueshift of both InN-like and AlN-like  $E_2$  phonons with decreasing In content is observed [Fig. 2(b)] in agreement with the theoretical predictions.<sup>14</sup> The  $E_2$  phonon frequencies versus In composition  $x$  can be approximated with

$$\omega_{E_2}^{\text{InN}}(x) = 647.5 - 159.6x - bx(1-x), \quad b = -102.7,$$

$$\omega_{E_2}^{\text{AlN}}(x) = 667.9 - 76.3x - bx(1-x), \quad b = 36.2, \quad (2)$$

with slightly larger bowing parameters  $b$  compared to theory.<sup>14</sup> The accuracy of the reported bowing parameters may in principle be limited by composition fluctuations. The full widths at half maximum of both AlN-like and InN-like  $E_2$  phonons, however, change only marginally ( $\sim 35\text{--}40 \text{ cm}^{-1}$ ) with varying the In composition in the nanocolumns indicating no major change in alloy disorder and/or compositional fluctuations for  $0.627 \leq x < 1$ .

In summary, we have calculated the lattice parameters of  $\text{In}_x\text{Al}_{1-x}\text{N}$  in the whole compositional range and obtained deviations from Vegard's rule,  $\delta_a = 0.0412 \pm 0.0039 \text{ \AA}$  and  $\delta_c = -0.060 \pm 0.010 \text{ \AA}$ , respectively. These deviations differ significantly from previous theoretical and experimental results.<sup>3,4</sup> Although small,  $\delta_a$  and  $\delta_c$  are shown to be important for improving the accuracy of XRD In content and are furthermore employed to estimate the In content in In-rich  $\text{In}_x\text{Al}_{1-x}\text{N}$  nanocolumns. The lattice parameters of these nanocolumns indicate virtually strain-free material. The  $E_2$  phonons in the  $\text{In}_x\text{Al}_{1-x}\text{N}$  nanocolumns are found to exhibit a two-mode behavior in agreement with theoretical predictions, and the compositional dependencies for the InN-like and AlN-like  $E_2$  frequencies are determined for  $\text{In}_x\text{Al}_{1-x}\text{N}$  with  $0.627 \leq x \leq 1$ .

The Swedish Research Council, VR Contract No. 2005-5054 and Linnaeus Grant, FCT Portugal (program Ciência 2007), and Swedish foundation for strategic research are gratefully acknowledged for financial support. One of the authors (I.A.A.) is grateful to Göran Gustafsson Foundation for Research in National Science and Medicine.

- <sup>1</sup>R. Butté, J.-F. Carlin, E. Feltin, M. Gonschorek, S. Nicolay, G. Christmann, D. Simeonov, A. Castiglia, J. Dorsaz, H. J. Buehlmann *et al.*, *J. Phys. D* **40**, 6328 (2007).
- <sup>2</sup>A. Dadgar, F. Schulze, J. Bläsing, A. Diez, A. Krost, M. Neuberger, E. Kohn, I. Daumiller, and M. Kunze, *Appl. Phys. Lett.* **85**, 5400 (2004).
- <sup>3</sup>B.-T. Liou, S.-H. Yen, and Y.-K. Kuo, *Appl. Phys. A: Mater. Sci. Process.* **81**, 651 (2005).
- <sup>4</sup>K. Lorenz, N. Franco, E. Alves, I. M. Watson, R. W. Martin, and K. P. O'Donnell, *Phys. Rev. Lett.* **97**, 085501 (2006).
- <sup>5</sup>T. Seppänen, L. Hultman, J. Birch, M. Beckers, and U. Kreissig, *J. Appl. Phys.* **101**, 043519 (2007).
- <sup>6</sup>V. Darakchieva, M. Beckers, M.-Y. Xie, L. Hultman, B. Monemar, J.-F. Carlin, E. Feltin, M. Gonschorek, and N. Grandjean, *J. Appl. Phys.* **103**, 103513 (2008).
- <sup>7</sup>G. Kresse and J. Furthmüller, *Phys. Rev. B* **54**, 11169 (1996).
- <sup>8</sup>A. V. Ruban and I. A. Abrikosov, *Rep. Prog. Phys.* **71**, 046501 (2008).
- <sup>9</sup>I. A. Abrikosov, S. I. Simak, B. Johansson, A. V. Ruban, and H. L. Skriver, *Phys. Rev. B* **56**, 9319 (1997).
- <sup>10</sup>W. Paszkowicz, R. Cerny, and S. Krukowski, *Powder Diffr.* **18**, 114 (2003).
- <sup>11</sup>H. Angerer, D. Brunner, F. Freudenberger, O. Ambacher, M. Stutzmann, R. Höpler, T. Metzger, E. Born, G. Dollinger, A. Bergmaier *et al.*, *Appl. Phys. Lett.* **71**, 1504 (1997).
- <sup>12</sup>J. Kamimura, T. Kouno, S. Ishizawa, A. Kikuchi, and K. Kishino, *J. Cryst. Growth* **300**, 160 (2007).
- <sup>13</sup>J. M. Calleja, S. Lasiç, J. Sanchez-Páramo, F. Agulló-Rueda, L. Cerutti, J. Ristiç, S. Fernández-Garrido, M. A. Sánchez-García, J. Grandal, E. Calleja *et al.*, *Phys. Status Solidi B* **244**, 2838 (2007).
- <sup>14</sup>H. Grille, C. Schmittler, and F. Bechstedt, *Phys. Rev. B* **61**, 6091 (2000).
- <sup>15</sup>A. Kasic, M. Schubert, J. Off, and F. Scholz, *Appl. Phys. Lett.* **78**, 1526 (2001).
- <sup>16</sup>V. M. Naik, W. H. Weber, D. Uy, D. Haddad, R. Naik, Y. V. Danylyuk, M. J. Lukitsch, G. A. Auner, and L. Rimai, *Appl. Phys. Lett.* **79**, 2019 (2001).
- <sup>17</sup>V. Darakchieva, P. P. Paskov, E. Valcheva, T. Paskova, B. Monemar, M. Schubert, H. Lu, and W. J. Schaff, *Appl. Phys. Lett.* **84**, 3636 (2004).